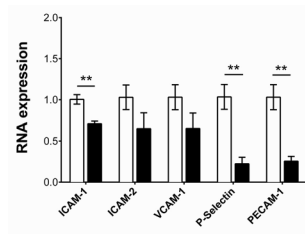
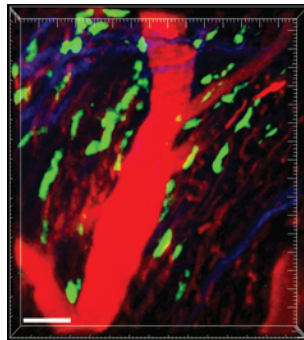


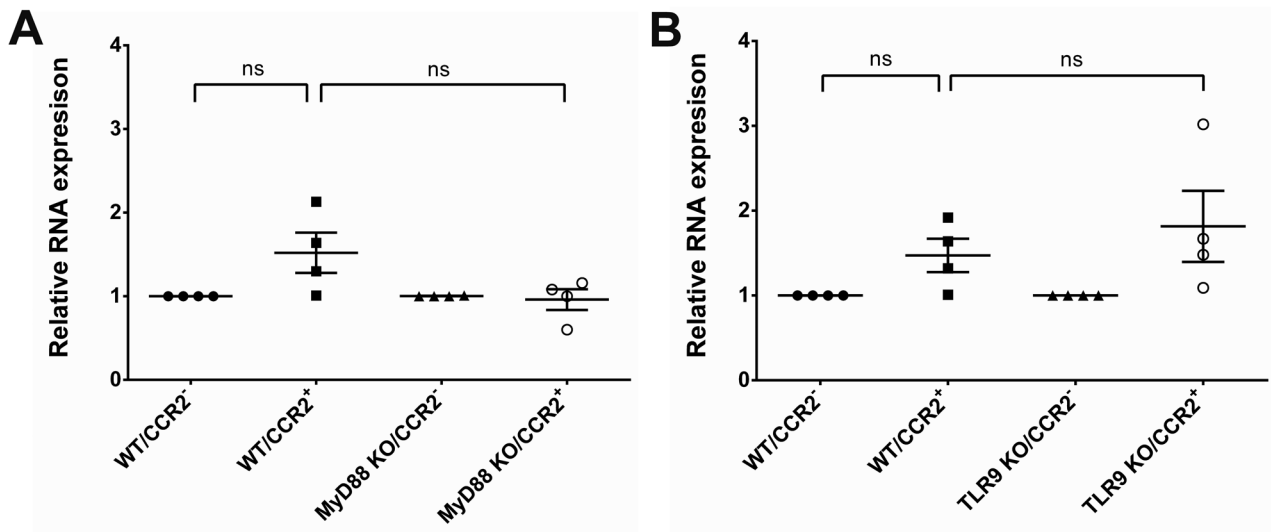
**Supplemental Figure 1. Depletion of CCR2<sup>+</sup> cells in hearts of CCR2-DTR mice after treatment with DT.**



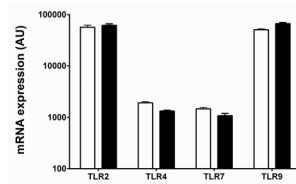
**Supplemental Figure 2. Expression levels of selectins and adhesion molecules in CD31<sup>+</sup> vascular endothelial cells in wildtype and MyD88-deficient heart grafts.**



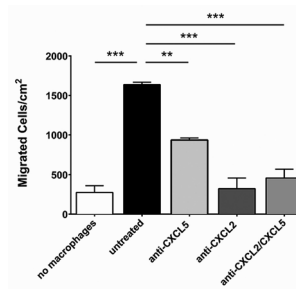
**Supplemental Figure 3. Tissue-resident macrophages in heart grafts.**



**Supplemental Figure 4.** Expression levels of CXCL1 in donor macrophage populations in wildtype, MyD88-deficient and TLR9-deficient heart grafts.



**Supplemental Figure 5.** Expression levels of Toll-Like Receptors in CCR2<sup>-</sup> and CCR2<sup>+</sup> macrophage populations in wildtype hearts.



**Supplemental Figure 6.** Cardiac CCR2<sup>+</sup> monocytes and monocyte-derived macrophages mediate neutrophil chemotaxis via CXCL2 and CXCL5 in vitro.

## Supplemental Information

### **Supplemental Figure 1. Depletion of CCR2<sup>+</sup> cells in hearts of CCR2-DTR mice after treatment with DT.**

Dot plots depict flow cytometric analysis of macrophage / monocyte populations in B6 CCR2 DTR heart after administration of saline (left) or DT (right). CCR2<sup>-</sup>MHC Class II<sup>hi</sup>, CCR2<sup>-</sup>MHC Class II<sup>low</sup>, CCR2<sup>+</sup> MHC Class II<sup>hi</sup> macrophages and CCR2<sup>+</sup>MHC Class II<sup>low</sup> monocytes are gated on hematopoietic (CD45<sup>+</sup>), myeloid (CD11b<sup>+</sup>CD64<sup>+</sup>) cells. Plots are representative of at least 3 independent experiments each with comparable results. Related to Figure 1.

### **Supplemental Figure 2. Expression levels of selectins and adhesion molecules in CD31<sup>-</sup> vascular endothelial cells in wildtype and MyD88-deficient heart grafts.**

Expression levels of P-selectin, ICAM-1, ICAM-2, VCAM-1 and PECAM in sorted vascular endothelial cells (CD45.2<sup>-</sup>CD45.1<sup>-</sup>CD31<sup>+</sup>) examined 2 hours after transplantation of B6 CD45.2<sup>+</sup> wildtype (white bars) or B6 CD45.2<sup>+</sup> MyD88-deficient (black bars) hearts into congenic B6 CD45.1<sup>+</sup> recipients. Results were normalized to 18sRNA and compared to CD31<sup>+</sup> vascular endothelial cells in wildtype hearts. \*\*P < 0.01 (unpaired t-test). Graph represents at least three separate experiments per group. Related to Figure 3.

### **Supplemental Figure 3. Tissue-resident macrophages in heart grafts.**

Intravital imaging of B6 LysM-GFP hearts two hours after transplantation into syngeneic hosts demonstrates numerous spindle-shaped Lyzzyme M<sup>+</sup> macrophages (green) in the interstitium of the grafts, many of which are adjacent to blood vessels (blood vessels appear red after injection of quantum dots). Scale bar: 50  $\mu$ m. Related to Figure 3.

### **Supplemental Figure 4. Expression levels of CXCL1 in donor macrophage populations in wildtype, MyD88-deficient and TLR9-deficient heart grafts.**

Expression levels of CXCL1 in sorted donor-derived (CD45.2<sup>+</sup>CD45.1<sup>-</sup>CD11b<sup>+</sup>CD64<sup>+</sup>) CCR2<sup>+</sup> and CCR2<sup>-</sup> macrophages examined 2 hours after transplantation of (A) B6 CD45.2<sup>+</sup> wildtype or B6 CD45.2<sup>+</sup> MyD88-deficient hearts into congenic B6 CD45.1<sup>+</sup> recipients and (B) B6 CD45.2<sup>+</sup> wildtype or B6 CD45.2<sup>+</sup> TLR9-deficient hearts into congenic B6 CD45.1<sup>+</sup> recipients. Results were normalized to 18sRNA and compared to the CCR2<sup>-</sup> macrophage population in each experimental group. ns= not significant (two-way ANOVA). Filled circles: wildtype CCR2<sup>-</sup> macrophages; filled squares: wildtype CCR2<sup>+</sup> macrophages and monocyte-derived macrophages; filled triangles: (A) MyD88-deficient or (B) TLR9-deficient CCR2<sup>-</sup> macrophages; open circles: (A) MyD88-deficient or (B) TLR9-deficient CCR2<sup>+</sup> macrophages and monocyte-derived macrophages. Graph represents four separate experiments per group where cells from two hearts were pooled for each experiment. Horizontal bars denote means and error bars denote SEM. Related to Figures 4 and 6.

**Supplemental Figure 5. Expression levels of Toll-Like Receptors in CCR2<sup>-</sup> and CCR2<sup>+</sup> macrophage populations in wildtype hearts.**

Quantitative RT-PCR assays demonstrating mRNA expression levels of TLR2, TLR4, TLR7 and TLR9 in CCR2<sup>-</sup> (MHC Class II<sup>low</sup> and MHC Class II<sup>hi</sup>) (white bars) and CCR2<sup>+</sup> MHC Class II<sup>hi</sup> (black bars) macrophage populations isolated from hearts of naïve B6 mice (n=4 mice). Related to Figure 5.

**Supplemental Figure 6. Cardiac CCR2<sup>+</sup> monocytes and monocyte-derived macrophages mediate neutrophil chemotaxis via CXCL2 and CXCL5 in vitro.**

In vitro chemotactic behavior of B6 neutrophils to CCR2<sup>+</sup>CD11b<sup>+</sup>CD64<sup>+</sup>CD45<sup>+</sup> monocytes and monocyte-derived macrophages isolated from B6 hearts. Experimental conditions include no addition of macrophages (white bar), untreated macrophage-neutrophil cultures (black bar) and treatment of macrophage-neutrophil cultures with CXCL5- (light gray bar) and CXCL2-neutralizing (dark gray bar) antibodies, alone or in combination. Graphs depict mean of migrated neutrophils derived from three individual experiments. Error bars denote SEM. \*\*P < 0.01; \*\*\*P < 0.001 (one-way ANOVA).

**Supplemental Movie 1. Time-lapse intravital two photon imaging of neutrophil behavior in heart grafts that have been harvested from wildtype donors that were treated with PBS-liposomes.**

Neutrophils (green) roll, adhere to the vessel wall, display intraluminal crawling and extravasate into myocardial tissue. Blood vessels (red) were labeled by intravenous injection of non-targeted 655-nm quantum dots. Scale bar: 50  $\mu$ m. Relative time is displayed in hrs:min:sec. Related to Figure 1.

**Supplemental Movie 2. Time-lapse intravital two photon imaging of neutrophil behavior in heart grafts that have been harvested from wildtype donors that were treated with clodronate liposomes.**

Neutrophils (green) roll and adhere to vessel wall, crawl slower, form intravascular clusters and do not extravasate efficiently. Blood vessels (red) were labeled by intravenous injection of non-targeted 655-nm quantum dots. Scale bar: 50  $\mu$ m. Relative time is displayed in hrs:min:sec. Related to Figure 1.

**Supplemental Movie 3. Time-lapse intravital two photon imaging of neutrophil behavior in heart grafts that have been harvested from wildtype donors and have received treatment with DT.**

Neutrophils (green) roll, adhere to the vessel wall, display intraluminal crawling and extravasate into myocardial tissue. Blood vessels (red) were labeled by intravenous

injection of non-targeted 655-nm quantum dots. Scale bar: 50  $\mu\text{m}$ . Relative time is displayed in hrs:min:sec. Related to Figure 2.

**Supplemental Movie 4. Time-lapse intravital two photon imaging of neutrophil behavior in heart grafts that have been harvested from CCR2 DTR donors and have received treatment with DT.**

Neutrophils (green) roll and adhere to vessel wall, crawl slower, form intravascular clusters and do not extravasate efficiently. Blood vessels (red) were labeled by intravenous injection of non-targeted 655-nm quantum dots. Scale bar: 50  $\mu\text{m}$ . Relative time is displayed in hrs:min:sec. Related to Figure 2.

**Supplemental Movie 5. Time-lapse intravital two photon imaging of neutrophil behavior in wildtype heart grafts.**

Neutrophils (green) roll, adhere to the vessel wall, display intraluminal crawling and extravasate into myocardial tissue. Blood vessels (red) were labeled by intravenous injection of non-targeted 655-nm quantum dots. Scale bar: 50  $\mu\text{m}$ . Relative time is displayed in hrs:min:sec. Related to Figure 3.

**Supplemental Movie 6. Time-lapse intravital two photon imaging of neutrophil behavior in MyD88-deficient heart grafts.**

Neutrophils (green) roll and adhere to vessel wall, form intravascular clusters, but do not extravasate efficiently. Blood vessels (red) were labeled by intravenous injection of

non-targeted 655-nm quantum dots. Scale bar: 50  $\mu\text{m}$ . Relative time is displayed in hrs:min:sec. Related to Figure 3.

**Supplemental Movie 7. Three-dimensional presentation of donor Lysozyme M<sup>+</sup> macrophages in donor hearts two hours after transplantation.**

Spindle-shaped macrophages (green) in donor LysM-GFP hearts 2 hours after transplantation into syngeneic wildtype mice. Blood vessels (red) were labeled by intravenous injection of non-targeted 655-nm quantum dots. Related to Figure 3.

**Supplemental Movie 8. Time-lapse intravital two photon imaging of neutrophil behavior in MyD88 floxed heart grafts.**

Neutrophils (green) roll, adhere to the vessel wall, display intraluminal crawling and extravasate into myocardial tissue. Blood vessels (red) were labeled by intravenous injection of non-targeted 655-nm quantum dots. Scale bar: 50  $\mu\text{m}$ . Relative time is displayed in hrs:min:sec. Related to Figure 3.

**Supplemental Movie 9. Time-lapse intravital two photon imaging of neutrophil behavior in heart grafts that lack MyD88 expression selectively in Lysozyme M<sup>+</sup> cells.**

Neutrophils (green) roll and adhere to vessel wall, form intravascular clusters, but do not extravasate efficiently. Blood vessels (red) were labeled by intravenous injection of



non-targeted 655-nm quantum dots. Scale bar: 50  $\mu$ m. Relative time is displayed in hrs:min:sec. Related to Figure 3.

**Supplemental Movie 10. Time-lapse intravital two photon imaging of neutrophil behavior in TLR2-deficient heart grafts.**

Neutrophils (green) roll, adhere to the vessel wall, display intraluminal crawling and extravasate into myocardial tissue. Blood vessels (red) were labeled by intravenous injection of non-targeted 655-nm quantum dots. Scale bar: 50  $\mu$ m. Relative time is displayed in hrs:min:sec. Related to Figure 5.

**Supplemental Movie 11. Time-lapse intravital two photon imaging of neutrophil behavior in TIRAP-deficient heart grafts.**

Neutrophils (green) roll, adhere to the vessel wall, display intraluminal crawling and extravasate into myocardial tissue. Blood vessels (red) were labeled by intravenous injection of non-targeted 655-nm quantum dots. Scale bar: 50  $\mu$ m. Relative time is displayed in hrs:min:sec. Related to Figure 5.

**Supplemental Movie 12. Time-lapse intravital two photon imaging of neutrophil behavior in TLR9-deficient heart grafts.**

Neutrophils (green) roll and adhere to vessel wall, crawl slower, form intravascular clusters, but do not extravasate efficiently. Blood vessels (red) were labeled by

intravenous injection of non-targeted 655-nm quantum dots. Scale bar: 50  $\mu$ m. Relative time is displayed in hrs:min:sec. Related to Figure 5.

**Supplemental Movie 13. Time-lapse intravital two photon imaging of neutrophil behavior in wildtype heart grafts after administration of isotype control antibody.**

Neutrophils (green) roll, adhere to the vessel wall, display intraluminal crawling and extravasate into myocardial tissue. Blood vessels (red) were labeled by intravenous injection of non-targeted 655-nm quantum dots. Scale bar: 50  $\mu$ m. Relative time is displayed in hrs:min:sec. Related to Figure 7.

**Supplemental Movie 14. Time-lapse intravital two photon imaging of neutrophil behavior in wildtype heart grafts after administration of CXCL2-neutralizing antibody.**

Neutrophils (green) fail to adhere to vessel wall. Blood vessels (red) were labeled by intravenous injection of non-targeted 655-nm quantum dots. Scale bar: 50  $\mu$ m. Relative time is displayed in hrs:min:sec. Related to Figure 7.

**Supplemental Movie 15. Time-lapse intravital two photon imaging of neutrophil behavior in CXCL5-deficient heart grafts.**

Neutrophils (green) roll and adhere to vessel wall, form intravascular clusters, but do not extravasate efficiently. Blood vessels (red) were labeled by intravenous injection of

non-targeted 655-nm quantum dots. Scale bar: 50  $\mu\text{m}$ . Relative time is displayed in hrs:min:sec. Related to Figure 7.